

## NRC Publications Archive Archives des publications du CNRC

### **The coordinated regulation of early meiotic stages is dominated by non-coding RNAs and stage-specific transcription in wheat**

Jiang, Yunfei; N'Diaye, Amidou; Koh, Chu Shin; Quilichini, Teagen D.; Shunmugam, Arun S. K.; Kirzinger, Morgan W.; Konkin, David; Bekkaoui, Yasmina; Sari, Ehsan; Pasha, Asher; Esteban, Eddi; Provart, Nicholas J.; Higgins, James D.; Rozwadowski, Kevin; Sharpe, Andrew G.; Pozniak, Curtis J.; Kagale, Sateesh

This publication could be one of several versions: author's original, accepted manuscript or the publisher's version. / La version de cette publication peut être l'une des suivantes : la version prépublication de l'auteur, la version acceptée du manuscrit ou la version de l'éditeur.

For the publisher's version, please access the DOI link below. / Pour consulter la version de l'éditeur, utilisez le lien DOI ci-dessous.

#### **Publisher's version / Version de l'éditeur:**

<https://doi.org/10.1111/tbj.16125>

*The Plant Journal*, pp. 1-16, 2023-01-29

#### **NRC Publications Archive Record / Notice des Archives des publications du CNRC :**

<https://nrc-publications.canada.ca/eng/view/object/?id=4c90e433-76de-45b6-b667-1c95057656b5>

<https://publications-cnrc.canada.ca/fra/voir/objet/?id=4c90e433-76de-45b6-b667-1c95057656b5>

Access and use of this website and the material on it are subject to the Terms and Conditions set forth at

<https://nrc-publications.canada.ca/eng/copyright>

READ THESE TERMS AND CONDITIONS CAREFULLY BEFORE USING THIS WEBSITE.

L'accès à ce site Web et l'utilisation de son contenu sont assujettis aux conditions présentées dans le site

<https://publications-cnrc.canada.ca/fra/droits>

LISEZ CES CONDITIONS ATTENTIVEMENT AVANT D'UTILISER CE SITE WEB.

**Questions?** Contact the NRC Publications Archive team at

PublicationsArchive-ArchivesPublications@nrc-cnrc.gc.ca. If you wish to email the authors directly, please see the first page of the publication for their contact information.

**Vous avez des questions?** Nous pouvons vous aider. Pour communiquer directement avec un auteur, consultez la première page de la revue dans laquelle son article a été publié afin de trouver ses coordonnées. Si vous n'arrivez pas à les repérer, communiquez avec nous à PublicationsArchive-ArchivesPublications@nrc-cnrc.gc.ca.

## RESOURCE

# The coordinated regulation of early meiotic stages is dominated by non-coding RNAs and stage-specific transcription in wheat

Yunfei Jiang<sup>1,†</sup>, Amidou N'Diaye<sup>2,†</sup>, Chu Shin Koh<sup>3,†</sup>, Teagen D. Quilichini<sup>1,†</sup>, Arun S. K. Shunmugam<sup>1</sup>, Morgan W. Kirzinger<sup>1</sup>, David Konkin<sup>1</sup>, Yasmina Bekkaoui<sup>1</sup>, Ehsan Sari<sup>1,2</sup>, Asher Pasha<sup>4</sup>, Eddi Esteban<sup>4</sup>, Nicholas J. Provart<sup>4</sup> , James D. Higgins<sup>5</sup>, Kevin Rozwadowski<sup>6</sup>, Andrew G. Sharpe<sup>3</sup>, Curtis J. Pozniak<sup>2,\*</sup> and Sateesh Kagale<sup>1,\*</sup> 

<sup>1</sup>Aquatic and Crop Resource Development, National Research Council Canada, 110 Gymnasium Place, Saskatoon, SK, S7N 0W9, Canada,

<sup>2</sup>Crop Development Centre, University of Saskatchewan, 51 Campus Drive, Saskatoon, SK, S7N 5A8, Canada,

<sup>3</sup>Global Institute for Food Security, University of Saskatchewan, 421 Downey Rd., Saskatoon, SK, S7N 4L8, Canada,

<sup>4</sup>Department of Cell and Systems Biology/Centre for the Analysis of Genome Evolution and Function, University of Toronto, 25 Willcocks St., Toronto, ON, M5S 3B2, Canada,

<sup>5</sup>Department of Genetics and Genome Biology, University of Leicester, Adrian Building, University Road, Leicester, Leicestershire, LE1 7RH, UK, and

<sup>6</sup>Saskatoon Research and Development Centre, Agriculture and Agri-Food Canada, 107 Science Pl., Saskatoon, SK, S7N 0X2, Canada

Received 14 October 2022; revised 20 January 2023; accepted 26 January 2023.

\*For correspondence (e-mail [curtis.pozniak@usask.ca](mailto:curtis.pozniak@usask.ca); [sateesh.kagale@nrc-cnrc.gc.ca](mailto:sateesh.kagale@nrc-cnrc.gc.ca)).

<sup>†</sup>These authors contributed equally to this work.

## SUMMARY

Reproductive success hinges on precisely coordinated meiosis, yet our understanding of how structural rearrangements of chromatin and phase transitions during meiosis are transcriptionally regulated is limited. In crop plants, detailed analysis of the meiotic transcriptome could identify regulatory genes and epigenetic regulators that can be targeted to increase recombination rates and broaden genetic variation, as well as provide a resource for comparison among eukaryotes of different taxa to answer outstanding questions about meiosis. We conducted a meiotic stage-specific analysis of messenger RNA (mRNA), small non-coding RNA (sncRNA), and long intervening/intergenic non-coding RNA (lincRNA) in wheat (*Triticum aestivum* L.) and revealed novel mechanisms of meiotic transcriptional regulation and meiosis-specific transcripts. Amidst general repression of mRNA expression, significant enrichment of ncRNAs was identified during prophase I relative to vegetative cells. The core meiotic transcriptome was comprised of 9309 meiosis-specific transcripts, 48 134 previously unannotated meiotic transcripts, and many known and novel ncRNAs differentially expressed at specific stages. The abundant meiotic sncRNAs controlled the reprogramming of central metabolic pathways by targeting genes involved in photosynthesis, glycolysis, hormone biosynthesis, and cellular homeostasis, and lincRNAs enhanced the expression of nearby genes. Alternative splicing was not evident in this polyploid species, but isoforms were switched at phase transitions. The novel, stage-specific regulatory controls uncovered here challenge the conventional understanding of this crucial biological process and provide a new resource of requisite knowledge for those aiming to directly modulate meiosis to improve crop plants. The wheat meiosis transcriptome dataset can be queried for genes of interest using an eFP browser located at [https://bar.utoronto.ca/efp\\_wheat/cgi-bin/efpWeb.cgi?dataSource=Wheat\\_Meiosis](https://bar.utoronto.ca/efp_wheat/cgi-bin/efpWeb.cgi?dataSource=Wheat_Meiosis).

**Keywords:** meiosis, transcriptome, small non-coding RNA, long intervening/intergenic non-coding RNA, isoform switching, wheat.

## INTRODUCTION

The regulated exchanges of meiosis ensure the fidelity and inherited genetic diversity of sexually reproducing species (Ma, 2006; Mercier et al., 2015; Yang et al., 2011). In particular, the exchange of genetic material through homologous recombination that occurs during meiotic prophase I requires chromatin remodeling, condensation, and the formation and then disassembly of the synaptonemal complex (Zickler & Kleckner, 2015). The non-random and highly structured organization of chromatin during prophase I creates hot and cold spots for recombination (Tock et al., 2021), and the breaking and reorganization of double-stranded DNA creates opportunities for the accumulation of mutations through mismatch and repair that may become fixed in subsequent generations. Evidence from model species suggests a tight regulation of meiotic progression by transcriptional, post-transcriptional, and epigenetic mechanisms that drive remodeling, with splice variants, long intervening/intergenic non-coding RNA (lincRNA), and small non-coding RNA (sncRNA) playing key, but poorly defined, roles. These may be distinct in different taxa or species (Bergero et al., 2021). In particular, plants have relatively large and complex epigenomes (Springer et al., 2015) that regulate chromatin remodeling and accessibility in all growth stages (Ahmad et al., 2010). Plants appear to harbor and employ a different and extended range of genomic sequence-based epigenetic modifications compared with animal and mammalian species (Feng et al., 2010), although, in practice, many of these regulatory elements and mechanisms have been discovered first in plants and later in non-plant species. To date, a global analysis of transcriptome complexity and the regulatory mechanisms operating in meiotic progression in plants is lacking.

In addition to extensive reorganization of meiotic chromatin architecture, crucial developmental and metabolic changes occur during the transition from vegetative to reproductive development in plants. Among these changes, decreased rates of transcription (Bergero et al., 2021; Geisinger et al., 2021) and elevated degradation of proteins and ribosomes (Dickinson & Heslop-Harrison, 1977) support the inhibition of cellular processes subsidiary to meiosis. Yet, the molecular mechanisms that remodel the cellular landscape and facilitate meiotic-phase transitions are largely unknown. Understanding the co-regulation of metabolic pathways in concert with meiotic transcriptional reorganization is essential to obtain a holistic view of meiotic differentiation.

Many important crop plants are polyploid. Wheat (*Triticum aestivum* L.), an allopolyploid formed from three ancestral grass genomes, is a crucial global food crop. In wheat, recombination during meiosis requires the recognition of homologous regions within sub-genomes for recombination to proceed, and the suppression of

homoeologous crossovers between the sub-genomes (Sears, 1977). Although at least two genes (Rey et al., 2017; Serra et al., 2021) involved in the suppression of homoeologous recombination, including the *Ph1* locus, are known, the pathway is not fully defined and the transcriptional network regulating homology recognition is largely unknown. This knowledge gap hampers efforts to increase available diversity using the gene pool available for wheat by wide crossing. Nevertheless, to date the polyploid recombination process is better understood in wheat than in other polyploids.

We proposed that a comprehensive dissection of the molecular regulation of meiosis in a crop plant could help identify target regulatory genes or epigenetic regulators that could be manipulated to support widespread efforts to increase recombination rates and broaden genetic variation to accelerate breeding and engineering (Stapley et al., 2017). We also aimed to describe the transcriptional landscape during meiosis in wheat as a first step to aid understanding of the distinctions in meiotic regulation between this and other plants, different ploidies, and other non-plant species.

Despite the subject's importance and the compelling reasons to investigate the regulation of meiosis in wheat, no such detailed studies examining the coordination of messenger RNAs (mRNAs) and non-coding RNAs (ncRNAs) at early meiosis stages in plants have been carried out previously, largely due to technical difficulties. In flowering plants, haploid male meiocytes are formed from pollen mother cells that are ensheathed by sporophytic cell layers of the anther wall (Goldberg et al., 1993; Ma, 2006). Efforts to profile the male meiotic transcriptome have therefore been limited by the use of whole anthers (Crismani et al., 2006; Martín et al., 2018). Using the MeioCapture method (Shunmugam et al., 2018) for attaining high-purity male meiocytes presented an opportunity to obtain synchronized populations of cells spanning the entire meiotic progression, including resolved cell populations in each of the five sub-stages of prophase I. In concert with Illumina and Oxford Nanopore platforms for in-depth coverage of mRNAs, sncRNAs, and lincRNAs, we aimed to capture a high-resolution network of the expressed transcripts and regulatory ncRNAs present throughout meiosis. This novel dataset enabled the complexity of the entire meiotic progression and its regulatory control elements to be analyzed in unprecedented detail. We uncovered (i) actively transcribed genes within the generally repressed transcriptional landscape of meiosis, including novel meiotic transcripts and sncRNAs, (ii) meiosis essential genes and regulatory modules, (iii) significant enrichment of sncRNAs and lincRNAs in meiocytes compared to non-meiotic tissues, and (iv) a negative correlation between the abundant meiotic sncRNAs and their target genes, implicating sncRNAs as key regulators in the reprogramming of central metabolic pathways subsidiary to meiosis,

including photosynthesis, glycolysis, hormone biosynthesis, cellular homeostasis, and ion and metal transport. Further, increased incidence of alternative splicing (AS) was not observed during meiosis in polyploid wheat, but evidence of transcript isoform switching was obtained. Our data support novel mechanisms regulating transcriptional dynamics during meiosis in wheat, including heightened transcriptional repression via sncRNA-mediated transcript degradation. We were also able to directly correlate expression patterns of ncRNAs with their target genes during meiosis for insights into the underlying mechanisms that regulate recombination and successful meiotic differentiation.

## RESULTS

### A wheat meiosis transcriptome atlas

Meiotic synchrony among stamens of a single floret allowed pure meiocytes from seven meiotic stages to be captured, including pre-meiotic G2 (Pm), the sub-stages of prophase I (termed leptotene [Le], zygotene [Zy], pachytene [Pa], and diplotene/diakinesis [Di]), metaphase I (MI), and metaphase II (MII) (Figure 1a). Using Illumina HiSeq2500 and Oxford Nanopore platforms, we generated 548 million paired-end short mRNA reads (137 Gb), 569 million small RNA reads, and 24 million long mRNA reads (24 Gb), respectively, from each developmental stage of the meiocytes, as well as the vegetative flag leaf (F; defined as the last leaf to emerge), young leaves (L), reproductive anthers (A), and pollen (P; Figure 1b,c; Table S1). The core meiosis transcriptome consisted of 9309 meiosis-specific transcripts (MSTs), 48 134 meiosis unannotated transcripts (MUTs), 1249 microRNAs (miRNAs), and 176 158 small interfering RNAs (siRNAs). Among the filtered reads mapped to the wheat reference genome (IWGSC v1.1), the meiotic transcriptome contained a higher percentage of reads aligned to non-coding regions, including untranslated regions (UTRs), introns, and intergenic regions, relative to the reads from vegetative and other reproductive materials (Figure 1d; Table S2).

Increased incidence of intergenic RNAs in meiocytes suggested the possibility of previously unidentified or unannotated transcripts that only accumulate during meiotic stages. We examined transcriptional units expressed within intergenic regions of the wheat genome and identified 48 134 MUTs. We classified the MUTs, identifying 11 121 coding transcripts with translatable open reading frames (ORFs) and 37 013 non-coding transcripts (Figure 1e). The majority of MUTs with ORFs had sequence homology to proteins in the non-redundant (nr) database (*E*-value cut-off of  $1E-10$ ). Among the non-coding transcripts, we distinguished miRNA precursors (Table S3) and other non-coding transcripts including ribosomal RNA (rRNA), transfer RNA (tRNA), small nucleolar RNA (snoRNA), spliceosomal RNA (Table S4), and a large proportion of lincRNAs (Figure 1e).

We found a general repression of mRNA transcription during meiosis, with significantly fewer genes expressed (transcripts per million [TPM] > 0.1 in at least two replicates) per unit length (5 Mb) across all wheat chromosomes in meiotic stages compared to vegetative and reproductive samples (Figure 1f,g) and a significantly higher proportion of genes expressed during prophase I relative to the other meiotic stages (Figure 1h). This comprehensive meiotic gene atlas provides a valuable resource for geneticists, and can be queried for genes of interest through the 'Electronic Fluorescent Pictograph' (eFP) browser at [https://bar.utoronto.ca/efp\\_wheat/cgi-bin/efpWeb.cgi?dataSource=Wheat\\_Meiosis](https://bar.utoronto.ca/efp_wheat/cgi-bin/efpWeb.cgi?dataSource=Wheat_Meiosis). The browser produces a fluorescent pictograph colored on the basis of transcript abundance data for individual wheat genes in meiotic stages and control tissues (exemplified in Figure S1).

### Dynamics of gene expression during meiotic prophase

To explore the dynamics of gene expression during meiosis, we identified wheat meiocyte differentially expressed transcripts (DETs) relative to the flag leaf control. Pair-wise comparisons throughout the progression of meiosis resulted in 29 344 DETs in meiocytes, of which 20 035 (68%) were downregulated and 9309 (32%) were upregulated, further supporting a general repression of transcription during meiosis (Figure 2a). Gene ontology (GO) terms that were enriched in the upregulated meiosis-specific DETs (MSTs), i.e., candidate processes enriched by meiosis-related gene activation, included DNA replication initiation, chromosome/chromatin organization, chromatin assembly or disassembly, cytoplasmic translation, and microtubule-based processes, as well as negative regulation of gene expression including RNA degradation (Figure S2a). Meiosis-specific downregulated genes included those for photosynthesis and multiple cellular metabolic process-related GO terms (Figure S2b).

The spatiotemporal coordination of upregulated genes in meiocytes was examined with a weighted gene co-expression network analysis (WGCNA; Langfelder & Horvath, 2008) that revealed 17 distinct co-expression modules, each containing between 65 and 1830 genes (Figure 2b,c). For the genes in each module, plotting mean expression across the stages of meiosis revealed predominant expression in either a single or a few related stages (Figure 2c), supporting *de novo* synthesis of transcripts during meiosis. Although relative upregulation could potentially have been accounted for by the global inactivation in meiocytes compared with flag leaves, instead there were striking patterns of co-expression (such as in modules 3–8) that could not be accounted for with a simple deactivation model. Together, these data supported unique and occasionally enhanced expression for a subset of genes in prophase I sub-stages (Figure 2c), rather than complete meiotic transcriptional inactivation.

4 Yunfei Jiang et al.

Of 115 wheat orthologs of known meiotic genes (Table S5), 56 transcripts belonging to 32 genes were differentially expressed in a meiosis stage-specific manner (Figure 2c; Figure S3). Among these 56 transcripts, eight had predicted functions in structural maintenance of

chromosome complexes (SMC1, 2, and 4; Figure 2c) – central regulators of chromosome dynamics, DNA replication, and DNA repair. The expression of SMC2 and SMC4 homeologs, which form heterodimers required for chromosome condensation in yeast and humans (Hirano, 2002; Jeppsson

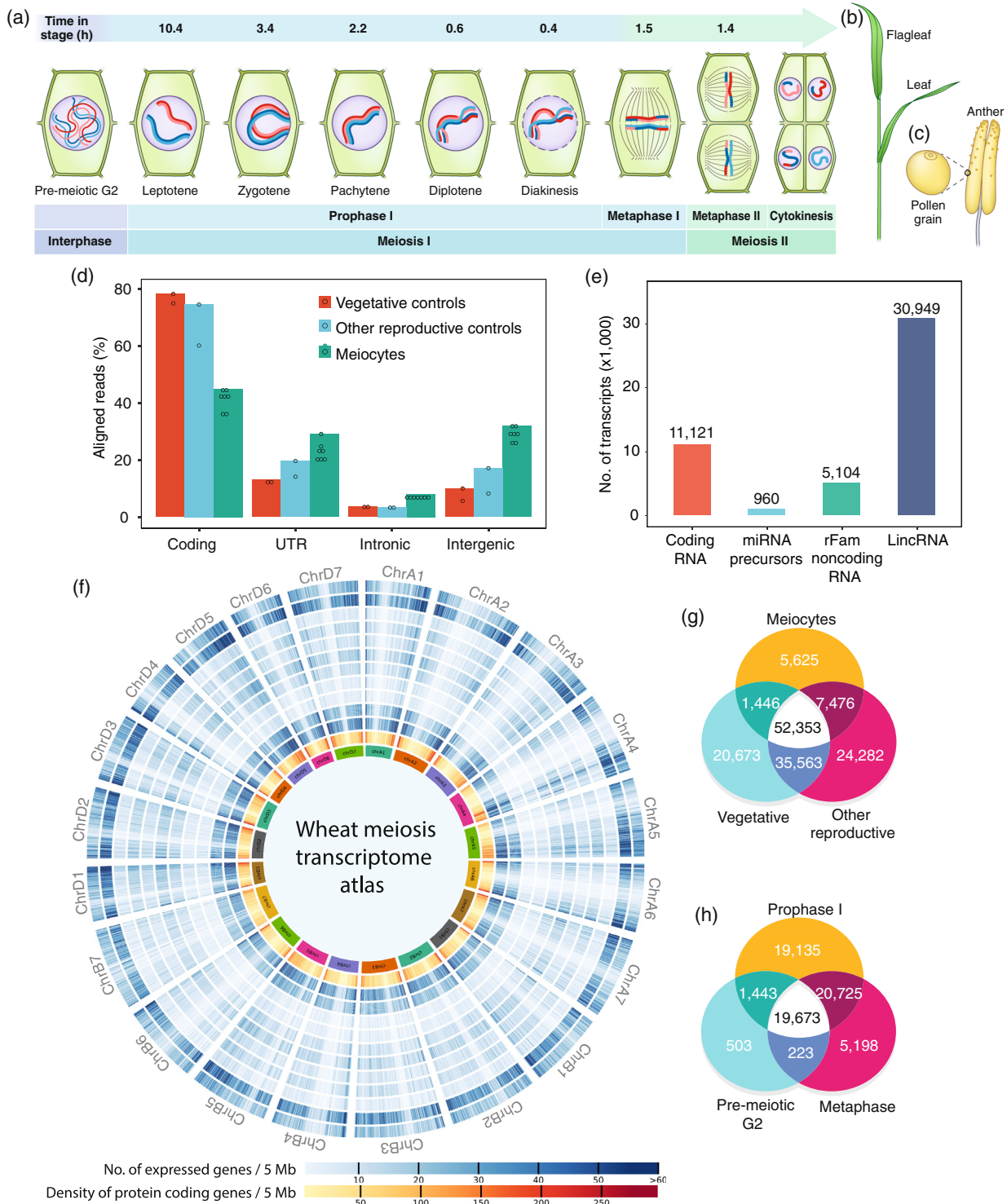


**Figure 1.** The transcriptome of male meiocytes during meiosis in wheat.

- (a) Diagrammatic representation of male meiocytes progressing through the cell cycle, from late interphase (left) through meiosis I and II (right). Key meiotic events are illustrated for a representative cell (green), as it transitions from a diploid pre-meiotic microspore mother cell (left) into the four haploid meiocytes of a microspore tetrad (right); its genetic information is represented by blue and red lines, and the nucleus is shown in gray.
- (b) Illustration of vegetative controls (leaf and flag leaf).
- (c) Illustration of reproductive controls (indehiscent anther and mature pollen).
- (d) Alignment of reads from meiocytes and vegetative and reproductive (non-meiotic) controls to genomic regions. Bars represent percentage of aligned reads falling within coding regions, UTRs, introns, and intergenic regions. The dot plot overlay shows the range of values observed in each meiosis stage or tissue category.
- (e) Categorization of novel transcripts from meiocyte intergenic regions into miRNA precursors, coding RNA, and long non-coding RNA by comparative sequence analysis.
- (f) Global patterns of gene expression in meiocytes and non-meiotic controls. The number of expressed genes per 5-Mb window is plotted for each chromosome (labeled along the outer periphery), with expression levels ranging from 0 to 60 genes/window scale represented by a blue-toned heatmap, as indicated by the scale. Each blue ring presents the expression profile of a specific tissue, starting with the leaf (innermost ring), followed by flag leaf, meiocytes in pre-meiotic G2, leptotene, zygotene, pachytene, diplotene/diakinesis, metaphase I, metaphase II, and then anther and pollen (outermost ring). Blue rings are segmented by chromosome (see windows) and contain a heatmap readout for up to 60 genes per chromosome segment. The internal orange track presents the density of protein-coding genes with 0–300 genes/window scale.
- (g) Venn diagram of transcript populations in meiocytes, vegetative controls, and reproductive controls.
- (h) Venn diagram of meiocyte transcript populations in the pre-meiotic G2 interphase, prophase I, and metaphase stages.

et al., 2014), was strongly correlated in mid-late stages of prophase I (from diplotene to diakinesis; Figure S3). The wheat orthologs of the *ASY1* gene, which is involved in axis morphogenesis and synaptonemal complex formation, were induced during leptotene and maintained expression throughout prophase I (Boden et al., 2009). The expression of the ortholog of another synaptonemal complex protein, *ZYP1*, was preferentially increased during late prophase I stages with the highest expression observed during pachytene and diplotene/diakinesis (Higgins et al., 2005). The expression of the ortholog of *SPO11-1*, which catalyzes double strand break (DSB) formation, peaked during zygotene (Grelon et al., 2001). Similarly, *HEI10* transcripts, involved in the Class I crossover (CO) pathway, were highly expressed in zygotene and pachytene (Chelysheva et al., 2012). The gene *SYN1/DIF1/REC8*, encoding sister chromatid cohesion protein 1 and involved in monopolar orientation of the kinetochore and DSB repair (Ma, 2006), had the highest expression in zygotene and pachytene among the seven stages of meiocytes (Figure S3). These results demonstrated a high degree of correlation of gene expression with the functions of a subset of known meiotic genes upregulated during meiosis.

We also found differences in transcript signatures among the homoeologous meiotic gene copies (Figure S3). For example, the *MUS81* gene copy on chromosome 3B had the lowest expression level in zygotene, whereas its homoeolog on chromosome 3D had the lowest expression level in the pre-meiotic G2 stage (Figure S3). We also found similar differences in transcript signatures among homoeologous gene copies of *AGO9/AGO104* on chromosomes 3A and 3D and *SMC2/CAP-E1* on chromosomes 3A, 3B, and 3D (Figure S3).

The expression patterns of more than 45% of previously uncharacterized MSTs and MUTs (4330 transcripts) were strongly correlated (Pearson correlation coefficient > 0.9) with the expression patterns of the known meiotic genes that were upregulated during meiosis (Table S6), suggesting a

possible role for these MSTs/MUTs in meiosis. The GO terms associated with these genes included histone-related mechanisms, actin crosslinking proteins, F-box family proteins, DNA packaging, cytoskeleton organization, supramolecular fiber organization, positive regulation of histone methylation, actin filament network formation, purine nucleobase transport, and cellular component disassembly (Table S7).

#### Altered splicing and isoform switching

AS is believed to play an important role during the transmeiotic progression of germ cells (Schmid et al., 2013) and in yeast and mouse testis a global increase in splicing is observed during meiosis (Juneau et al., 2007; Schmid et al., 2013). Further, differential transcript usage, known as isoform switching, can impact the adaptive functionality of genes, with transcriptional toggling between mRNA isoforms known to drive protein level changes during meiosis (Cheng et al., 2018). To assess the incidence of AS during meiosis, patterns of expression for meiotic AS variants (ASVs) were compared with vegetative and reproductive controls. Despite the dramatic differences observed in the numbers of genes expressed, the average number of exons per gene model was near identical among meiocytes and controls (Table S8), containing the same proportions of ASVs in the four major classes distinguished: intron retention, alternative acceptor sites, alternative donor sites, and exon skipping (Table S9). In contrast to yeast and mouse testis, no significant differences ( $P > 0.05$ , analysis of variance [ANOVA]) in meiosis-specific patterns of AS were identified. However, isoform switching was observed in 44 upregulated genes during meiosis (Figure 3a). We tracked differential expression patterns between select transcript pairs throughout meiosis to temporally distinguish isoform switch events (Figure 3b–e). Among the known meiotic genes, the isoforms of *MEIOSIS ARRESTED AT LEPTOTENE 1* (*MEL1*; TraesCS2D02G176500), which encodes a meiosis regulatory Argonaute (AGO) protein that binds

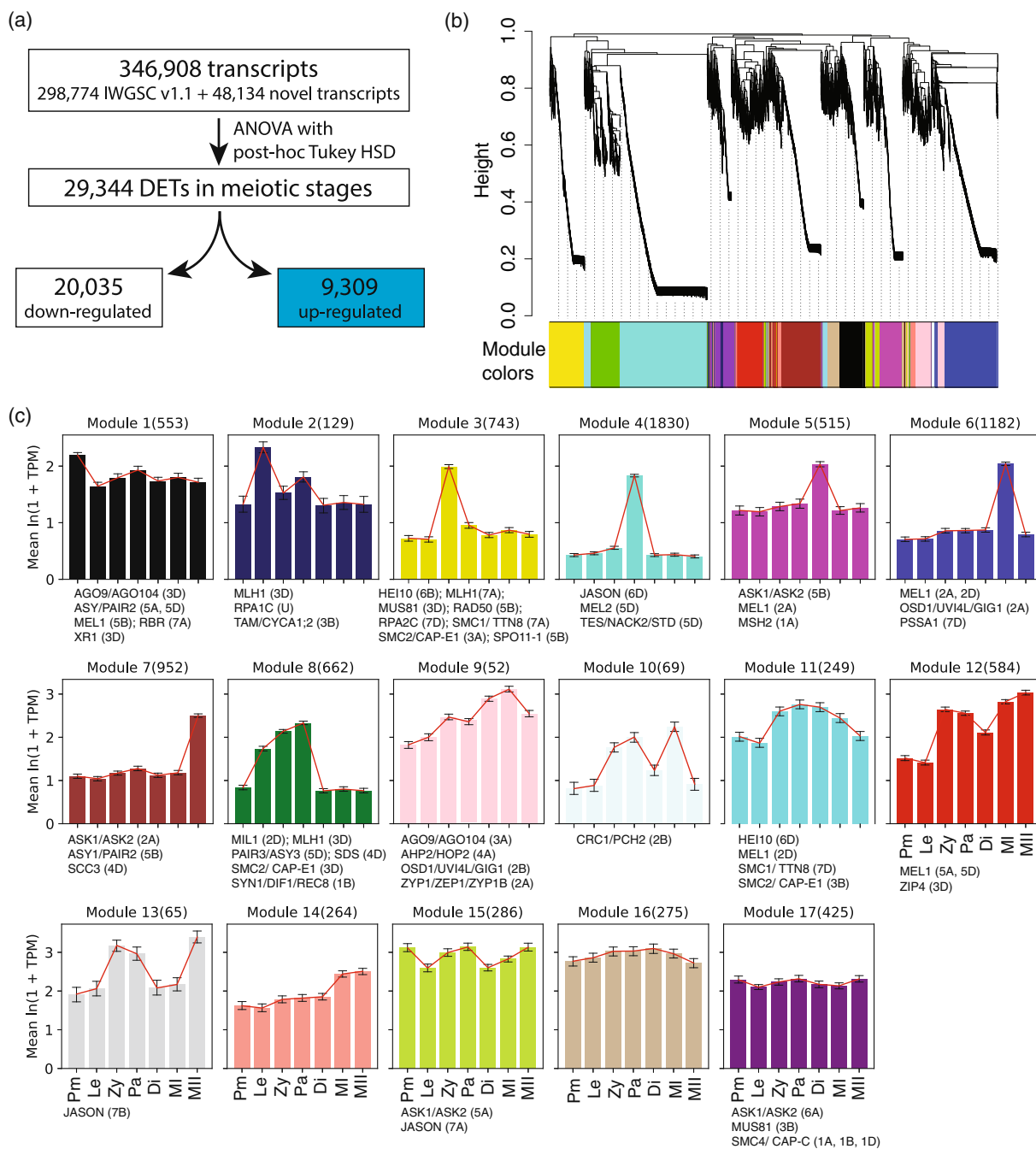


**Figure 2.** Weighted gene co-expression network analysis of upregulated meiotic genes.

(a) The differential expression analysis (ANOVA followed by post-hoc Tukey HSD test) identified 9309 upregulated and 20 035 downregulated transcripts during meiosis. The expression of genes in different meiotic stages was compared to flag leaf (control). DETs, differentially expressed transcripts.

(b) Dendrogram showing co-expression modules identified by weighted gene co-expression network analysis of upregulated genes during meiosis. The major tree branches constitute 17 distinct co-expression modules labeled by different colors.

(c) Tissue specificity of meiotic genes belonging to individual co-expression modules. Histogram bars are colored according to the corresponding module color. The histograms show the mean and standard deviation for the transformed expression values (mean over replicates of  $\ln(1 + \text{TPM})$ ) for each tissue. The number of genes in each module is indicated in parentheses. Known meiotic genes belonging to individual modules are listed below. Pm, pre-meiotic G2; Le, leptotene; Zy, zygotene; Pa, pachytene; Di, diplotene/diakinesis; MI, metaphase I; MII, metaphase II.

phased secondary small interfering RNAs (phasiRNAs, germ cell-specific sncRNAs) and mediates target gene cleavage during prophase I (Lian et al., 2021), showed isoform

switching (Figure 3b). Of the two differentially expressed isoforms of *MEL1*, TraesCS2D02G176500.1 was specifically upregulated during metaphase I, whereas

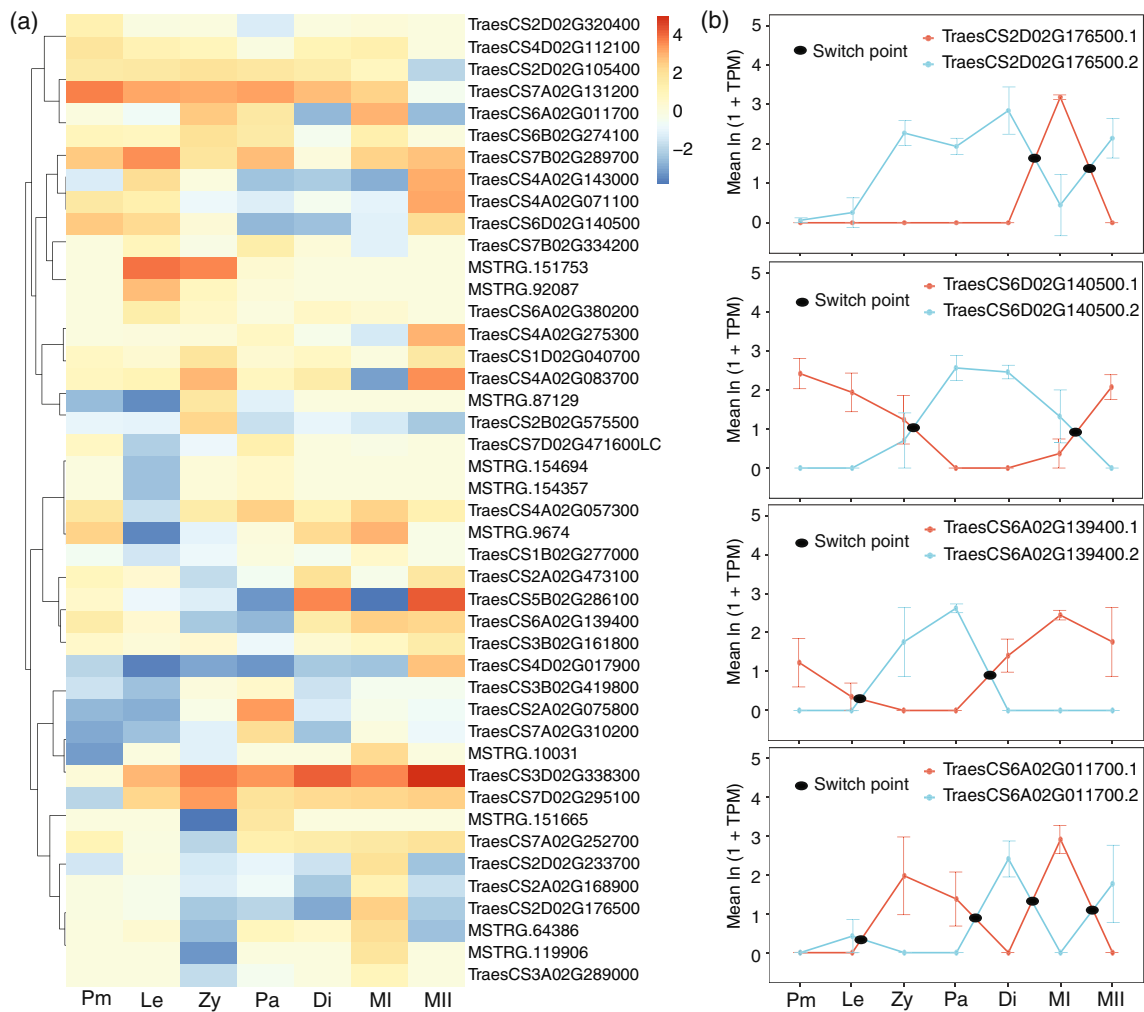


**Figure 3.** Alternate use of mRNA isoforms during meiosis in wheat.

(a) Heatmap of relative TPM levels of 44 isoform pairs showing isoform switch events. Ratios were calculated as  $\ln(\text{TPM}(\text{isoform 1}/\text{isoform 2}))$ .

(b) Line plots showing examples of transcript pairs with an isoform switch event at different time points. Each data point represents the mean  $\pm$  standard error of expression values from three biological replicates. Pm, pre-meiotic G2; Le, leptotene; Zy, zygotene; Pa, pachytene; Di, diplotene/diakinesis; MI, metaphase I; MII, metaphase II.

TraesCS2D02G176500.2 was downregulated during metaphase I but upregulated during prophase I stages (Figure 3b). These data suggested differential functional potential for select gene isoforms in a non-canonical mode of gene regulation.

### Regulatory non-coding RNA landscape

To investigate the sncRNA landscape during meiosis, the size, distribution, abundance, and characteristics of sncRNAs expressed in meiocytes were determined. A total of 177 407 distinct sncRNAs were expressed (cumulative read count > 100) in meiocytes and controls (Table S10), consisting of 1249 sncRNAs annotated as miRNAs (processed from single-stranded precursor RNA and containing a hairpin structure) and 176 158 sncRNAs annotated as siRNAs (produced from DICER/DICER-like processing of double-stranded RNAs). Of

the expressed miRNAs, 661 were previously identified plant miRNAs and 588 were novel (Table S10).

In contrast to the repressed transcriptional landscape observed for meiotic mRNA profiles, sncRNAs were highly abundant in meiocytes relative to control tissues (Figure 4a). The number of sncRNAs expressed in pre-meiotic G2 was higher compared to leptotene. However, there was a gradual increase in the number of sncRNAs expressed in prophase I stages, with the highest number of sncRNAs expressed during pachytene (Figure 4a). Of the 120 236 sncRNAs expressed during meiosis, 78 412 (65%) were uniquely expressed in meiocytes relative to vegetative and other reproductive controls (Figure 4b), and the majority of meiotic sncRNAs were expressed in prophase I (Figure 4c). Throughout meiosis, 21- and 24-nucleotide sncRNAs were the most abundant (Figure 4d).

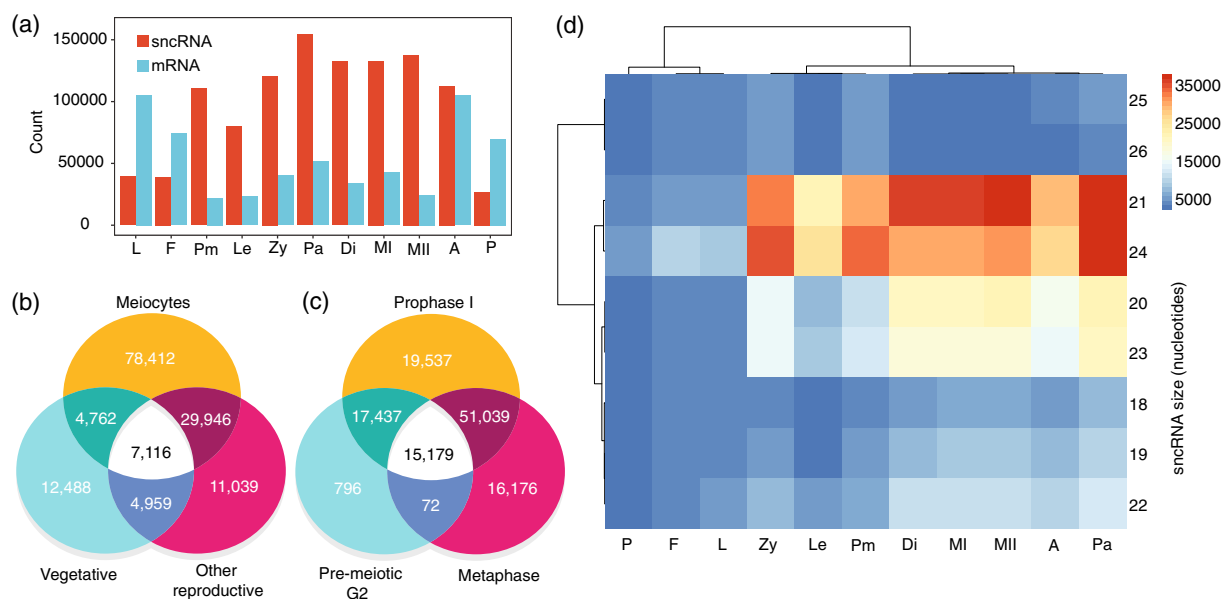


**Figure 4.** An overview of sncRNA expression in meiotic and non-meiotic tissues.

(a) The number of mRNAs and sncRNAs expressed in meiotic and non-meiotic tissues. Pm, pre-meiotic G2; Le, leptotene; Zy, zygotene; Pa, pachytene; Di, diplotene/diakinesis; MI, metaphase I; MII, metaphase II; L, leaf; F, flag leaf; P, pollen; A, anther.  
 (b) Venn diagram illustrating distinct and overlapping sncRNA populations in meiocytes, vegetative controls, and reproductive controls.  
 (c) Venn diagram illustrating distinct and overlapping sncRNA populations in the pre-meiotic G2 interphase, prophase I, and metaphase.  
 (d) Size distribution of sncRNAs and their abundance in meiotic and non-meiotic tissues.

### sncRNAs specifically target genes involved in photosynthesis, glycolysis, and other subsidiary metabolic processes during meiosis

ncRNAs have critical and diverse roles in the regulation of gene expression (Chen, 2009; Statello et al., 2021). Considering the abundance of sncRNAs in meiocytes identified here, we sought to understand the role of these ncRNAs. First, differentially expressed miRNAs and siRNAs were identified using the flag leaf as a reference. The majority of differentially expressed sncRNAs were upregulated, with 686 upregulated miRNAs, 197 downregulated miRNAs, 121 341 upregulated siRNAs, and 19 162 downregulated siRNAs (Figure S4). Next, the relationship between sncRNAs with differential expression in meiocytes and the expression of their putative target mRNAs was examined using psRNAtarget software to identify putative mRNA targets. Pearson correlation coefficients for all miRNA–mRNA and siRNA–mRNA pairs were computed as the estimation of correlations (Figure 5a,b) and expression profiles analyzed across meiotic stages and vegetative and reproductive controls. The transcriptional activity of the majority of miRNAs (75%) and siRNAs (70%) was negatively correlated with that of their putative target mRNAs (Figure 5a,b). This suggested roles for sncRNAs in the repression of transcription, either through the repression of expression or increased degradation of target mRNAs.

To explore the functional relevance of putative sncRNA–mRNA interactions, tissue-wise means and variances of

transformed expression values were plotted for miRNA or siRNA and their putative target mRNAs (Figure 5c,d). Contrasting expression patterns for miRNA or siRNA and their putative target mRNAs were observed in meiocytes across their development. GO terms enriched for putative targets from differentially expressed miRNA and siRNAs during meiosis included processes related to metabolism, transport of ions and metals, chemical and cellular homeostasis, hormone biosynthesis, photosynthesis, and glycolysis (Figure 5e,f), suggesting that mRNAs associated with these processes were regulated by sncRNAs and repressed during meiosis.

### Dynamics of lincRNA during meiotic prophase

lincRNAs act as *cis*- or *trans*-regulators of gene expression through interactions with transcriptional machinery proteins or chromatin-modifying complexes, or as the precursors of sncRNAs (Geisinger et al., 2021; Liu et al., 2015; Taylor et al., 2015). The largest proportion of novel transcripts identified in meiocytes here consisted of lincRNAs (Figure 1e). We performed differential expression analysis using ANOVA followed by post-hoc Tukey's honest significant difference (HSD) test for pair-wise comparisons between flag leaf control and different meiotic stages for the 30 949 lincRNAs identified. This substantially narrowed the lincRNAs to 1798 with differential expression in meiocytes, consisting of 1584 upregulated and 217 downregulated lincRNAs relative to the flag leaf (Figure S4). For the upregulated lincRNAs,

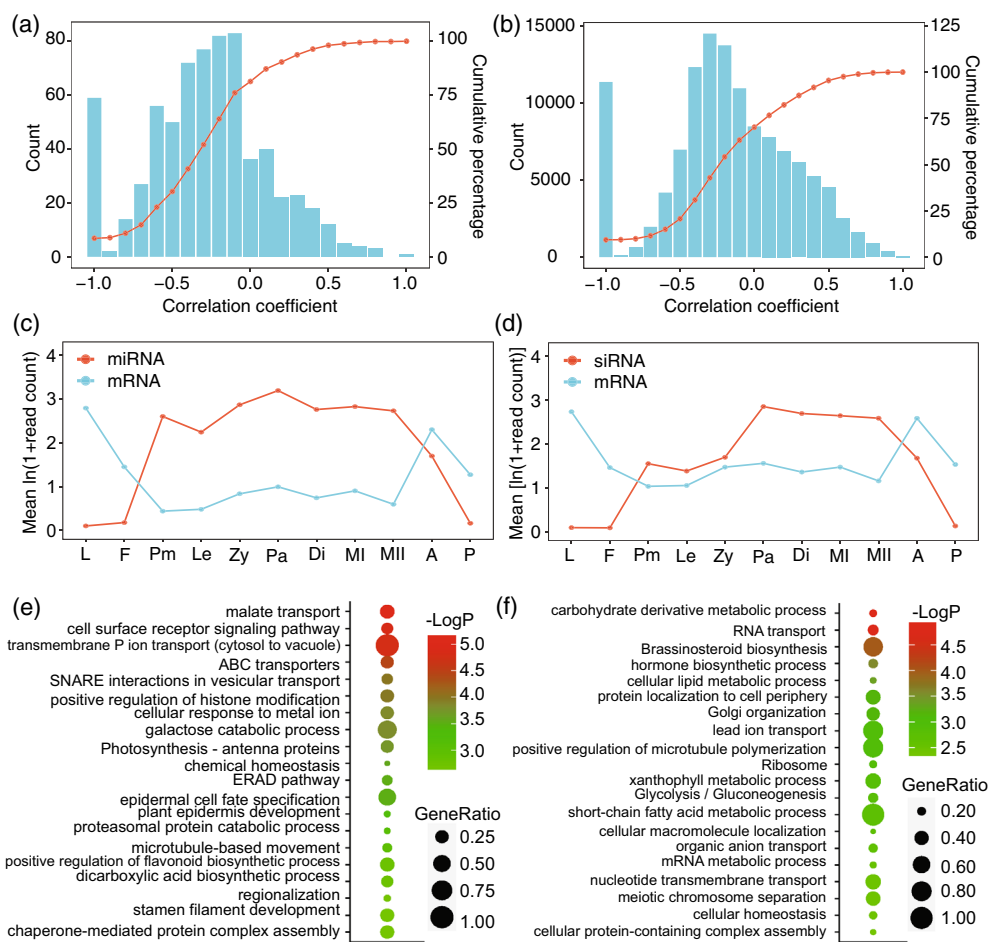


**Figure 5.** Negative relationship between the expression profiles of sncRNAs and their target mRNAs.

- (a) Histogram of correlation coefficients calculated by comparing the expression patterns of upregulated miRNAs in meiotic tissues and their putative mRNA targets. A cumulative frequency plot is overlaid on the histogram.
- (b) Histogram of correlation coefficients calculated by comparing the expression patterns of upregulated siRNAs in meiotic tissues and their putative mRNA targets. A cumulative frequency plot is overlaid on the histogram.
- (c) Line plots showing the mean expression values of miRNAs and their target mRNAs with negative correlation coefficient values.
- (d) Line plots showing the mean expression values of siRNAs and their target mRNAs with negative correlation coefficient values.
- (e) Gene ontology (GO) term enrichment in putative gene targets of miRNAs. The heatmap depicts the top 20 enriched GO categories.
- (f) GO term enrichment in putative gene targets of siRNAs. The heatmap depicts the top 20 enriched GO categories.

WGCNA identified eight modules consisting of 71 to 727 co-expressed lincRNAs (Figure 6a,b). The plots of tissue-wise means and variances of transformed TPM values for lincRNA belonging to each module revealed lincRNAs in modules had stage-specific expression patterns, either predominantly expressed in an individual meiotic stage (as in modules 1 through 7) or expressed in a narrow range of early meiosis (as in module 8; Figure 6b). The distinct, restricted expression pattern for lincRNAs across meiosis suggested that lincRNAs may play a role in the demarcation of key transitions in meiotic progression in wheat.

lincRNAs can act as local regulators influencing the expression of neighboring protein-coding genes (Engreitz et al., 2016; Ørom et al., 2010; Wang et al., 2011). To test whether meiotic lincRNAs affected the expression of

nearby genes, we compared the expression patterns of the lincRNAs upregulated in meiosis relative to flag leaf, with those of their 40 adjoining genes (determined as the 20 genes upstream and downstream of each lincRNA). Pearson correlation coefficients for the expression patterns of all lincRNA–mRNA neighbor pairs revealed a majority of lincRNAs were positively correlated with the expression of adjoining genes, particularly for neighbors in the immediate vicinity of each lincRNA (Figure 6c). These data indicate a substantial fraction of meiotic lincRNAs positively influenced the expression of their gene neighbors.

## DISCUSSION

The ordered progression of meiosis requires extensive reconfiguration of chromatin architecture to ensure

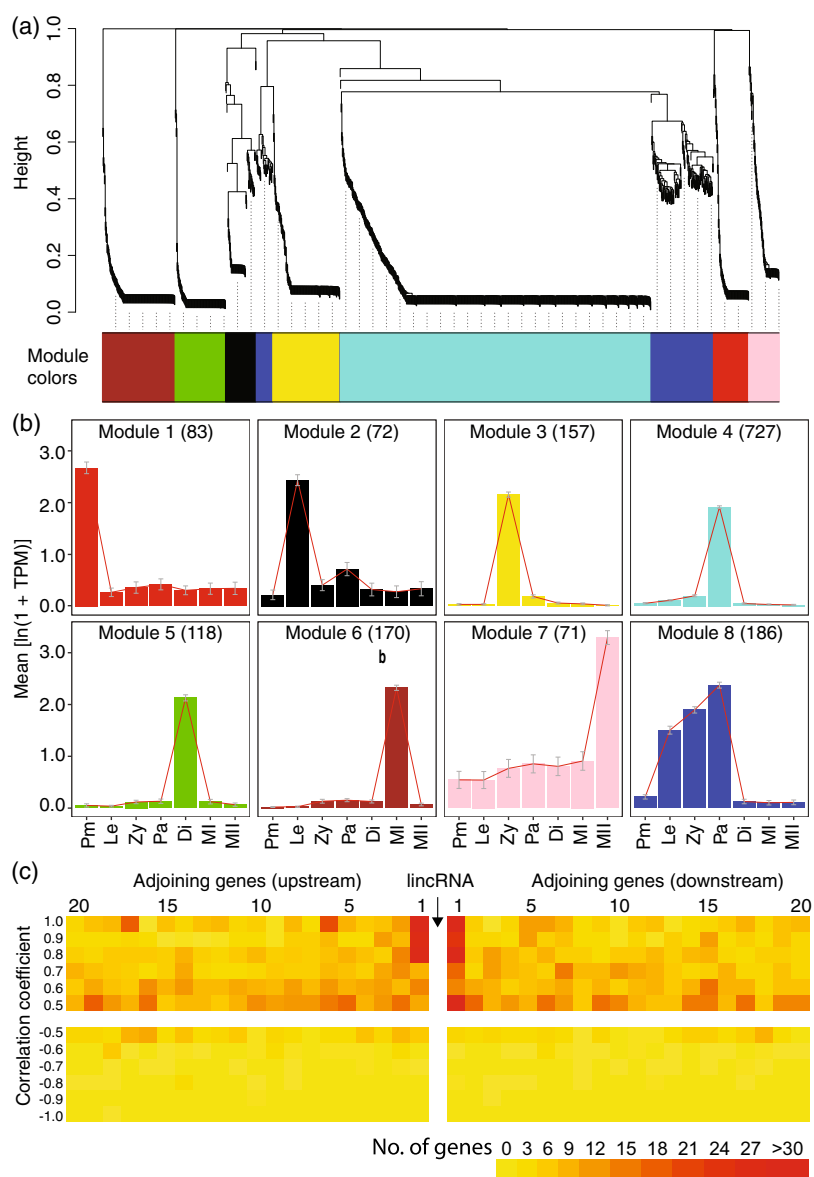


**Figure 6.** Tissue-specific co-expression networks of lincRNAs.

(a) Hierarchical cluster tree showing eight modules identified by WGCNA of 1584 lincRNAs upregulated in different meiotic stages.

(b) Tissue specificity of lincRNAs belonging to individual co-expression modules. Histogram bars colored according to the corresponding module color show the mean and standard deviation for the transformed expression values. The number of genes in each module is indicated in parentheses. Pm, pre-meiotic G2; Le, leptotene; Zy, zygotene; Pa, pachytene; Di, diplotene/diakinesis; MI, metaphase I; MII, metaphase II.

(c) Local regulation of gene expression by lincRNAs. The expression patterns of lincRNAs and adjoining genes (20 genes upstream and 20 genes downstream) were compared. The heatmap shows the numbers of genes with correlation coefficient values greater than 0.5 (positive correlation with corresponding lincRNA) and lower than  $-0.5$  (negative correlation).

accurate segregation of the genome into gametes (Bergero et al., 2021). Owing to the extreme condensation of chromatin during meiosis, transcription appears to be largely inactivated during the progression of meiosis in higher eukaryotes (Bergero et al., 2021). Here, the isolation of purified and stage-specific wheat male meiocytes, paired with in-depth sequencing of coding RNA and ncRNA, revealed the transcriptional landscape during meiosis in wheat. The resulting data challenge the notion of a largely inert,

repressed transcriptional landscape associated with condensed chromatin and displaced transcription factors. Amidst global repression, a variety of upregulated coding RNAs and ncRNAs with distinct spatiotemporal patterns of expression were detected, supporting a central role for select transcript populations in orchestrating meiotic progression in plants. Among these, we found an increased incidence of expression of previously unannotated transcriptional units. Similar observations were also made in

yeast, where MUTs that accumulate only during meiotic development were discovered (Lardenois et al., 2011). A substantial proportion of previously uncharacterized genes were co-expressed in a phase-specific manner together with known meiotic genes. Together, these data support the unique and occasionally enhanced expression of a larger subset of genes than previously described.

In contrast, a minority of known meiotic genes were differentially expressed in a meiosis stage-specific manner in wheat. A similar observation in barley (*Hordeum vulgare*) identified only 28 known meiotic genes with differential expression across meiosis (Barakate et al., 2021). In Arabidopsis, 29 of the 68 genes known to be involved in meiosis exhibited preferential expression during meiosis (Chen et al., 2010). This is probably because DNA repair genes are likely to be required during mitosis and meiosis, but meiosis-specific proteins like ASY1 and ZYP1 are not. The lack of meiosis-specific expression of many known meiotic genes here is most likely due to their overlapping functions in mitosis and meiosis, similarly to the *ZYP1* meiotic gene, which was also found to be abundantly expressed in late bud development stages 15–18 in Arabidopsis (Higgins et al., 2005; Klepikova et al., 2016).

The GO terms associated with MSTs having strong correlation with known meiotic genes included many with potential functions in epigenetic regulation of chromatin, structural modifications, and DSB repair. It has been well documented that histone modifications mediate meiotic events, including chromosome structural modifications, chromatin remodeling, and dynamic transcriptional regulation during meiosis (Wang et al., 2017). F-box proteins are also involved in meiotic differentiation. A previous study showed that meiotic F-box proteins are essential for DNA DSB repair and are active during leptotene and pachytene of prophase I in rice (*Oryza sativa*) (He et al., 2016). Although the direct role of actin crosslinking proteins in meiosis is unclear, they are essential for organizing actin filaments into subcellular scaffolds that play important roles in cellular motility and adhesion (Tseng et al., 2005). The spatiotemporal expression patterns combined with co-expression networks presented here provide a valuable foundation for future experiments aimed at understanding the meiotic functions of the yet uncharacterized MSTs.

To further challenge long-held assumptions about the processes that regulate meiosis in eukaryotes, this study identified elevated incidences of isoform switching, rather than AS, in wheat male meicytes relative to controls. Although a high proportion of reads aligned to UTRs, introns, and intergenic regions in meicytes, suggesting a high incidence of alternatively spliced transcripts in meiotic tissues relative to vegetative controls, the average number of exons per gene model and proportions of variants across the major AS classes remained near constant between meicytes and controls. Despite a lack of

evidence for elevated AS in meiotic wheat meicytes, the isoform switching detected indicates differential transcript usage may similarly function to alter protein accumulation during meiosis. Additionally, our finding that alternative isoforms of a number of genes, such as the gene encoding the phasiRNA-binding MEL1 (TraesCS2D02G176500), are overexpressed at specific stages of meiosis and switch with phase transitions strongly suggests a role for these alternative isoforms in regulating meiotic transitions, in agreement with recent findings in meiotic *Brassica rapa* pollen (Golicz et al., 2021).

Regulatory ncRNAs, including sncRNAs (20–24 nucleotides) and lincRNAs (>200 nucleotides), play essential roles in the coordinated progression of cellular differentiation (Bélanger et al., 2020; Böhmdorfer & Wierzbicki, 2015; Dai et al., 2019; Goh et al., 2015; Gou et al., 2014; Huang et al., 2019). lincRNAs function in chromatin modification, the regulation of DNA, histone methylation, and nucleosome positioning (Böhmdorfer & Wierzbicki, 2015). The elevated expression of lincRNAs in plant and animal reproductive organs, including the meicytes of sunflower (*Helianthus annuus*), implies a role for these ncRNAs in regulating gene expression during meiosis (Flórez-Zapata et al., 2016). Our data show that a substantial fraction of meiotic lincRNAs positively influenced the expression of their gene neighbors, suggesting that lincRNAs may assist in maintaining the expression of select genes in the overall condensed chromosome environment of meiosis.

In our samples, 24-nucleotide siRNAs were the most abundant among sncRNAs, and this is consistent with previous reports in diverse plants (Lunardon et al., 2020), including wheat, where 24-nucleotide siRNAs constituted the largest proportion of sncRNAs in spike, seed, and seedling tissues (Li et al., 2014); 24-nucleotide siRNAs regulate expression and chromatin, in particular heterochromatin, via the recruitment and spread of RNA-directed DNA methylation (RdDM), often to silence repetitive elements (Fultz et al., 2015). Their relative over-abundance in meicytes in our study may indicate a role in the generalized suppression of transcription during meiosis, especially in the highly repetitive wheat genome. Moreover, 21-nucleotide sncRNAs were also overrepresented in meiosis compared with vegetative tissues. In Arabidopsis, 21-nucleotide sncRNAs are produced from post-transcriptionally degraded transposable elements in pollen vegetative cells and move into sperm cells to inhibit harmful transposition in the next generation (Martínez et al., 2016), but their relative over-abundance in meicytes compared with pollen here suggested another role. They may also be produced from sites near DSBs (Hawley et al., 2017) and important for their repair and meiotic recombination (Bélanger et al., 2020; Huang et al., 2019; Lunardon et al., 2020), as may 21- or 24-nucleotide phasiRNAs, consistent with their presence at the meiotic stages in our study.

In addition to their role in heterochromatin condensation and the prevention of repetitive element transposition, 24-nucleotide siRNAs have been shown to repress the expression of target coding genes in (non-phase-specific) meiocytes in the male lineage of *Arabidopsis* via RdDM (Walker et al., 2018). Here, co-analysis of expression patterns for coding RNAs and ncRNAs in meiotic stages and correlation of ncRNAs with their putative targets showed that the transcription levels for the majority of upregulated miRNAs and siRNAs during meiosis were negatively correlated with the transcript levels of their putative target mRNAs, indicating that these sncRNAs may function as regulators of targeted meiotic mRNA repression. The mRNAs identified as sncRNA targets were enriched in metabolism-related processes, suggesting an important role for sncRNAs in downregulating genes involved in cellular processes that are subsidiary to meiosis. The decay of mRNA and ethylene-responsive element binding factor-associated amphiphilic repression (EAR)-motif-mediated transcriptional repression may also play a role in the regulation of mRNA abundance during meiosis as several genes involved in RNA decay pathways and genes encoding EAR-motif-containing transcriptional repressors were upregulated in a meiosis stage-specific manner (Figure S5; Table S11). These analyses provide insight into the dynamic RNA interactions that orchestrate gene expression during meiosis. Uncovering the molecular impacts of ncRNA regulators on corresponding mRNA targets and the transcriptional landscape during meiosis will be an important next step in uncovering the mechanisms regulating meiosis in plants.

The recombination of maternal and paternal DNA during meiosis is critical for the production of genetically diversified offspring. With the rate of recombination governed, in part, by specific genetic loci, uncovering the molecular basis of meiotic recombination provides opportunities to target meiotic recombination rates and accelerate the development of novel germplasm for plant breeding (Stapley et al., 2017). Our dissection of the meiocyte transcriptome in polyploid wheat revealed a subset of meiosis-expressed essential genes and gene regulatory mechanisms with the potential to direct future efforts to increase recombination frequencies and assist wild trait introgression into cultivated plants.

## EXPERIMENTAL PROCEDURES

### Plant materials and growing conditions

Wheat ( $2n = 6x = 42$ , AABBDD) genotype Chinese Spring was planted with two seeds per pot in four-inch pots filled with Sunshine Gro® mix (Seba Beach, AB, Canada). All plants were grown in a growth chamber (PGW40; Conviron, Winnipeg, MB, Canada) at the National Research Council Canada (Saskatoon, SK, Canada) with a constant temperature of  $21 \pm 1^\circ\text{C}$ , a photoperiod of 16 h (day)/8 h (night), and a minimum photosynthetic photon flux density of  $400 \mu\text{mol m}^{-2} \text{sec}^{-1}$  during the day. Plants were monitored daily, watered regularly, and treated every 2 weeks using

water-soluble 20-20-20 fertilizer at a rate of  $3.0 \text{ g L}^{-1}$  and chelated micronutrient mix at a rate of  $0.3 \text{ g L}^{-1}$  (both from Plant Products Co. Ltd., Brampton, ON, Canada).

### Meiocyte isolation

Meiocytes were isolated from anthers in developing wheat inflorescences using the MeioCapture method (Shunmugam et al., 2018). Briefly, the spikes were collected along with the leaf sheath, placed in a beaker with distilled water on ice, and transferred to the lab immediately for meiocyte isolation. Individual florets were excised from the spikelets and placed in  $1 \times$  Dulbecco's phosphate-buffered saline (DPBS) buffer (ThermoFisher Scientific, Minneapolis, MN, USA; Catalog no. 14190144). Three of the five anthers from each floret, with filament of stamens detached, were isolated and placed in  $50 \mu\text{l}$   $1 \times$  DPBS solution for use as the reproductive control. This was repeated to collect a minimum of 50 anthers, which were sorted by length using a dissection scope fitted with an ocular micrometer. Indehiscent anthers ranging from 0.7 to 1.2 mm were used. One anther from each floret was squished and stained with 15–20  $\mu\text{l}$  of 2% acetocarmine to allow the meiotic stage to be determined by light microscopy. The sporogenous archesporial columns containing meiocytes (meiocyte-filled sacs) were extracted from the remaining two anthers of each floret by nicking the narrow end of the anther in the DPBS dome and rolling a dissecting needle along the anther towards the nick. These steps were repeated until 5000–7000 meiocytes per replicate were collected for each meiotic stage, including pre-meiotic G2, leptotene, zygotene, pachytene, diplotene/diakinesis, metaphase I, and metaphase II (Figure 1a). The meiocytes were stored in RNAlater solution (ThermoFisher; Catalog no. AM7020) prior to RNA isolation. Other plant tissues, including young leaf (approximately 2 weeks after seeding), flag leaf (the last leaf to emerge, immediately below the spike), whole anthers (0.6–1.2 mm in length), and pollen grains (immediately after anther dehiscence) were collected (Figure 1b,c) for comparison. At least three independent biological replicates were collected for each tissue or meiotic stage.

### RNA isolation and sequencing

Total RNA from meiocytes and control tissues was isolated using the RNAqueous™-Micro Total RNA Isolation Kit (ThermoFisher Scientific; Catalog no. AM1931) according to the manufacturer's instructions. The RNA yield and purity were assessed using a Nanodrop 1100 (ThermoFisher Scientific), and RNA integrity was evaluated using an Agilent 2100 Bioanalyzer (Agilent Technologies, Santa Clara, CA, USA). TruSeq RNA and small RNA sequencing libraries were constructed following the manufacturer's instructions (Illumina, San Diego, CA, USA; <http://www.illumina.com/>) and sequenced (up to 125 cycles) using an Illumina HiSeq2500 platform.

### Oxford Nanopore cDNA library preparation and sequencing

RNA sequencing libraries were generated from the isolated RNA of six samples, including leaf, pre-meiotic and meiotic anthers, and pre-meiotic and meiotic meiocytes, according to the manufacturer's instructions. Briefly, 100 ng of RNA from each sample was reverse transcribed to obtain strand-switched DNA which was assessed for quantity and quality using a Qubit fluorometer. Each sample was then end-prepared for barcode ligation. After the barcodes were ligated, the samples were quantified and pooled for adapter ligation. The final library pool was quantified and

sequenced using FLO-MIN106 flow cells with R9 chemistry on an Mk1B MinION.

### mRNA expression profiling

Before read mapping, short Illumina reads were filtered using Trimmomatic (v0.39) (Bolger et al., 2014) with default settings by trimming adapter and low-quality sequences and removing reads shorter than 75 bp. Filtered reads were aligned to the wheat reference genome (IWGSC v1.1; IWGSC, 2018) using STAR (v2.7.5a; Dobin et al., 2013). Transcript abundance was estimated using the RSEM (v1.3.3) algorithm (Li & Dewey, 2011) and the IWGSC v1.1 annotation, and the expected read counts and TPM values, which normalize counts to a consistent number per library (1 million) to facilitate the comparison of relative expression across various samples (Wagner et al., 2012), were generated. TPM values were transformed by adding one and taking the natural logarithm to meet the statistical assumption of normal data distribution (Kagale et al., 2016). The transformed values were used in the subsequent analyses. Genes with a TPM greater than 0.1 in at least two biological replicates were considered as expressed genes. The similarity between biological replicates was assessed by calculating pair-wise Pearson correlation coefficients ( $R$ ) for each meiotic stage or tissue type. The average  $R$ -values for meiotic stages were slightly lower (0.81) compared to vegetative (0.94) and other reproductive (0.88) tissues (Table S12). RNA sequencing analysis of meiotic stages was repeated with three additional replicates, which produced  $R$ -values that were similar to the first set (Table S13). Similar observations were also made in transcriptome studies of maize (*Zea mays*) and other plant species (Dukowic-Schulze et al., 2014). The low  $R$ -values could be the result of residual fragments produced by mRNA decay during meiosis. The circular plots representing expression profiles of genes were drawn using the web-based Accusyn browser (<https://accusyn.usask.ca/>).

### Oxford Nanopore data filtering and analysis

Oxford Nanopore Sequencing reads were base-called using Guppy (v3.6.0) and then demultiplexed into individual samples using deepbiner (v0.2.0). Porechop (v0.24) was used to trim remaining sequencing adapters and NanoFilt (v2.7.0) was used to quality-trim reads to a minimum quality score of 7. Trimmed reads were aligned to the CS reference genome in a splice-aware manner using minimap2 (version 2.17-r941) (Li, 2018) with the parameter '-ax splice'. IsoQuant (v1.0.0) was used to identify known and novel transcripts in minimap2 alignment files. Oxford Nanopore Technologies open-source script (spliced\_bam2gff) was used to convert the bam alignment to gff files.

### Annotation of novel transcripts expressed during meiosis

To investigate the possibility of unannotated transcripts among intergenic RNAs, annotations for the transcriptional units expressed in intergenic regions of the wheat genome were generated using StringTie (v2.1.1) (Pertea et al., 2015). Among the 48 134 novel transcripts identified, transcript classifications were assigned using CPC2 (v2) (Kang et al., 2017), CNIT (Guo et al., 2019), BLAST (v2.9.0; Altschul et al., 1990), and TransDecoder (v5.5.0) (TransDecoder, 2018), which identified 11 121 coding transcripts with translatable ORFs and 37 013 non-coding transcripts (Figure 1e).

### Differential expression and co-expression analyses

The analysis of statistical significance of differences in gene expression between the meiotic stages, vegetative tissues, and

other reproductive tissues in CS was performed using ANOVA. Pair-wise comparisons between flag leaf and remaining tissues or meiotic stages were made using the post-hoc Tukey HSD test.  $P$ -values were adjusted using the Benjamini–Hochberg correction for multiple testing (Benjamini & Hochberg, 1995). A false discovery rate-adjusted  $P$ -value less than 0.05 was deemed statistically significant. To identify clusters of highly correlated genes (with similar expression patterns) in meiotic stages, a co-expression network was constructed for the 9309 upregulated transcripts using the WGCNA (v1.69) R package (Langfelder & Horvath, 2008). Clustering was performed with  $\ln(1 + \text{TPM})$  values with a soft thresholding power of 12. The minimum number of genes in each module (minModuleSize) was set to 30. The maximum number of genes in one block (maxBlockSize) was set to 10 000. The hierarchical clustering tree was cut using the Dynamic Hybrid Tree Cut algorithm with mergeCutHeight set to 0.25. For comparison, an inventory of known meiotic genes in Arabidopsis and rice was compiled (Table S5) (Capilla-Perez et al., 2018; Ma, 2006; Wang et al., 2014) and wheat orthologs were identified using Ensembl plants (release 49; Yates et al., 2020) with default settings.

### sncRNA analysis

Low-quality reads and sequencing adapters were removed. Reads longer than 17 nucleotides were retained for analysis. Reads were aligned to the wheat reference genome (IWGSC v1.1; IWGSC, 2018) using Bowtie (v2.4.4; <http://bowtie.cbcb.umd.edu>) (Langmead et al., 2009) with the accepted number of mismatches set to zero. The number of sequencing reads for each sncRNA was normalized to 10 million total reads per library based on the sequencing depth. sncRNAs with normalized read counts greater than 10 reads in at least two biological replicates were considered expressed. The similarity between biological replicates was assessed by calculating pair-wise Pearson correlation coefficients ( $R$ ) for each meiotic stage or tissue type (Table S14). For the identification of conserved miRNAs, the sncRNA sequences were queried using the rFam database (a comprehensive collection of ncRNAs) for tRNA-/rRNA-/snoRNA-derived sequences (Kalvari et al., 2018); the remaining sequences were mapped against the miRbase database (release 22) to identify annotated miRNAs. For the identification of novel miRNAs, putative miRNAs were predicted using miRDeep-P2 (<https://sourceforge.net/projects/mirdp2/>) (Kuang et al., 2019), which identified 698 unique miRNA sequences (2365 pre-miRNA genomic loci) based on read alignment and secondary structure prediction using RNAfold. Differential expression of sncRNAs was performed using ANOVA as described above.

Potential targets of sncRNAs were searched using the program psRNatarget (2017 update) (Dai et al., 2018). Selection was based on the smallest 'Expectation' value. The best matched target mRNAs were used for subsequent analysis, and global correlation analysis of sncRNAs and their best target mRNA expression patterns was performed.

### Differential AS analysis

The Astalavista (v4.0) tool asta (Foissac & Sammeth, 2007) was used to identify AS variants for wheat transcripts expressed in different meiotic stages. Analysis of AS isoform switch events was performed using the default TSIS R package (Guo et al., 2017) and meiotic transcripts with upregulated expression across seven meiotic stages (including pre-meiotic G2, leptotene, zygotene, pachytene, diplotene/diakinesis, metaphase I, and metaphase II).

## GO analysis

GO enrichment analysis was conducted using Metascape (Zhou et al., 2019) with default settings. Prior to Metascape analysis, wheat transcript IDs were converted to their Arabidopsis ortholog IDs using Ensembl Plants BioMart (Yates et al., 2020) with default parameters. Due to the limit of 3000 genes as input for the Metascape analysis, the topmost downregulated genes were selected based on the criteria of adjusted  $P \leq 0.001$  and an absolute difference of  $\text{mean}(\ln(1 + \text{TPM}))$  between target tissue and flag leaf  $\geq 1.6$ , resulting in 2918 Arabidopsis gene IDs.

## Statistical analysis

All statistical methods and tests used in this study are described in the text and figure legends as appropriate.

## AUTHOR CONTRIBUTIONS

SK, CJP, AGS, and KR conceived the research and designed experiments. YJ, ASKS, YB, and ES performed experiments and generated sequencing data. JDH provided cytogenetics and microscopy training. YJ, AN, CSK, TDQ, SK, MWK, and DK performed data analysis. AP, EE, and NJP developed the eFP Browser. TDQ, YJ, and SK prepared figures and wrote the manuscript. All authors read and approved the final manuscript.

## ACKNOWLEDGMENTS

Debbie Maizels at Zoobotanica, UK (<http://www.scientific-art.com/>) is gratefully acknowledged for providing Figure 1 artwork. We would like to thank Venkatesh Bollina, Parul Jain, Vera Cekic, and Jodi Therres for assistance with meiocyte isolation and microscopy and other technical support. We gratefully acknowledge the funding support from Genome Prairie, Genome Canada, the Western Grains Research Foundation, the Saskatchewan Ministry of Agriculture, the Saskatchewan Wheat Development Commission, and the Alberta Wheat and Barley Development Commission through the Canadian Triticum Applied Genomics<sup>2</sup> (CTAG<sup>2</sup>) project. Funding was also provided by the National Research Council Canada through the Canadian wheat improvement flagship program. AGS and CSK were supported by the Global Institute for Food Security Plant Improvement Program and the Canada First Research Excellence Fund through the Designing Crops for Global Food Security Initiative at the University of Saskatchewan.

## CONFLICT OF INTEREST

The authors declare that they have no competing interests.

## DATA AVAILABILITY STATEMENT

The raw sequencing data and processed transcriptome data (sample metadata, read counts, and TPM values) have been deposited into the National Center for Biotechnology Information Gene Expression Omnibus under accession number GSE182171 (<https://www.ncbi.nlm.nih.gov/geo/query/acc.cgi?acc=GSE182171>). RNA sequencing data as TPM were also made available in the Wheat eFP Browser at [https://bar.utoronto.ca/efp\\_wheat/cgi-bin/efpWeb.cgi?dataSource=Wheat\\_Meiosis](https://bar.utoronto.ca/efp_wheat/cgi-bin/efpWeb.cgi?dataSource=Wheat_Meiosis). Briefly, data were databased on the Bio-Analytic Resource for Plant Biology (Toufighi et al., 2005) and

images and XML files specific for a Wheat Meiosis view were generated as described (Winter et al., 2007).

## SUPPORTING INFORMATION

Additional Supporting Information may be found in the online version of this article.

**Figure S1.** eFP browser view of expression changes during meiosis in wheat. Exemplary wheat meiosis eFP browser images showing expression patterns of SPO-11-1 (a) and TraesCS1B02G461800.1 (b). SPO11-1 is a meiosis-specific gene with significantly elevated expression during zygotene. TraesCS1B02G461800.1 is specifically expressed in leaf and flag leaf but downregulated in meiotic stages. In both cases, red indicates higher expression and yellow indicates lower expression.

**Figure S2.** Gene ontology enrichment analysis of differentially expressed genes during meiosis. A heatmap of the 20 most statistically enriched terms colored by hypergeometric  $P$ -values is shown. Prior to the Metascape analysis (<https://metascape.org/>), wheat transcript IDs were converted to their Arabidopsis ortholog IDs using Ensembl Plants BioMart with default parameters. (a) Genes upregulated during meiosis. (b) Genes downregulated during meiosis.

**Figure S3.** Gene expression patterns of differentially expressed known meiotic genes in wheat (identified based on orthology to Arabidopsis and rice meiotic genes). Putative gene names, chromosome number (in brackets), and the co-expression module number (see Figure 2c) to which individual gene belongs are shown. TPM, transcripts per million; Pm, pre-meiotic G2; Le, leptotene; Zy, zygotene; Pa, pachytene; Di, diplotene; MI, metaphase I; MII, metaphase II.

**Figure S4.** Differential expression analysis of sncRNA and lincRNA. (a) The differential expression analysis of miRNAs identified 686 upregulated and 197 downregulated miRNAs during meiosis. The expression of miRNAs in different meiotic stages was compared to flag leaf (control). (b) The differential expression analysis of siRNAs identified 121 341 upregulated and 19 162 downregulated siRNAs during meiosis. The expression of siRNAs in different meiotic stages was compared to flag leaf (control). (c) The differential expression analysis of lincRNAs identified 1584 upregulated and 217 downregulated lincRNAs during meiosis. The expression of lincRNAs in different meiotic stages was compared to flag leaf (control).

**Figure S5.** Expression patterns of RNA decay genes. Module-wise (Figure 2c) distribution of differentially expressed wheat orthologs of known RNA decay genes. The letter in each colored block indicates the module number to which the RNA decay gene belongs.

**Table S1.** Summary statistics for transcriptome sequencing of meiotic stages and control tissues.

**Table S2.** Read alignment statistics.

**Table S3.** Classification of novel transcripts (miRNA precursors) expressed during meiosis.

**Table S4.** Classification of novel transcripts (rRNAs, tRNAs, snoRNAs, and spliceosomal RNAs) expressed during meiosis.

**Table S5.** Wheat orthologs of known meiotic genes.

**Table S6.** Correlation coefficients calculated by comparing the expression patterns of differentially expressed known meiotic genes and co-regulated meiosis-specific transcripts (MSTs).

**Table S7.** GO term enrichment in meiosis-specific transcripts (MSTs) that have high correlation with the expression pattern of known meiotic genes.

**Table S8.** Alternative splicing events during meiosis compared to vegetative tissues.

**Table S9.** Frequency of different alternative splicing events in individual meiotic stages and vegetative tissues.

**Table S10.** sncRNA landscape (1249 miRNAs and 176 158 siRNAs) of meiosis.

**Table S11.** Meiotic differentially expressed transcription factors with conserved ethylene-responsive element binding factor-associated amphiphilic repression (EAR) motif sequence.

**Table S12.** Pearson correlation between biological replicates 1, 2, and 3 (mRNA).

**Table S13.** Pearson correlation between biological replicates 4, 5, and 6 (mRNA).

**Table S14.** Pearson correlation between biological replicates 1, 2, and 3 (sncRNA).

## REFERENCES

- Ahmad, A., Zhang, Y. & Cao, X.F. (2010) Decoding the epigenetic language of plant development. *Molecular Plant*, **3**, 719–728.
- Altschul, S.F., Gish, W., Miller, W., Myers, E.W. & Lipman, D.J. (1990) Basic local alignment search tool. *Journal of Molecular Biology*, **215**, 403–410.
- Barakate, A., Orr, J., Schreiber, M., Colas, I., Lewandowska, D., McCallum, N. *et al.* (2021) Barley anther and meiocyte transcriptome dynamics in meiotic prophase I. *Frontiers in Plant Science*, **11**, 1–24.
- Bélangier, S., Pokhrel, S., Czymmek, K. & Meyers, B.C. (2020) Premeiotic, 24-nucleotide reproductive phasiRNAs are abundant in anthers of wheat and barley but not rice and maize. *Plant Physiology*, **184**, 1407–1423.
- Benjamini, Y. & Hochberg, Y. (1995) Controlling the false discovery rate: a practical and powerful approach to multiple testing. *Journal of the Royal Statistical Society, Series B*, **57**, 289–300.
- Bergero, R., Ellis, P., Haerty, W., Larcombe, L., Macaulay, I., Mehta, T. *et al.* (2021) Meiosis and beyond – understanding the mechanistic and evolutionary processes shaping the germline genome. *Biological Reviews*, **96**, 822–841.
- Boden, S.A., Langridge, P., Spangenberg, G. & Able, J.A. (2009) TaASY1 promotes homologous chromosome interactions and is affected by deletion of Ph1. *The Plant Journal*, **57**, 487–497.
- Böhmendorfer, G. & Wierzbicki, A.T. (2015) Control of chromatin structure by long noncoding RNA. *Trends in Cell Biology*, **25**, 623–632.
- Bolger, A.M., Lohse, M. & Usadel, B. (2014) Trimmomatic: a flexible trimmer for Illumina sequence data. *Bioinformatics*, **30**, 2114–2120.
- Capilla-Perez, L., Solier, V., Portemer, V., Chambon, A., Hurel, A., Guillebaux, A. *et al.* (2018) The HEM lines: a new library of homozygous *Arabidopsis thaliana* EMS mutants and its potential to detect meiotic phenotypes. *Frontiers in Plant Science*, **9**, 1–9.
- Chelysheva, L., Vezon, D., Chambon, A., Gendrot, G., Pereira, L., Lemhemdi, A. *et al.* (2012) The Arabidopsis HEI10 is a new ZMM protein related to Zip3. *PLoS Genetics*, **8**, e1002799.
- Chen, C., Farmer, A.D., Langley, R.J., Mudge, J., Crow, J.A., May, G.D. *et al.* (2010) Meiosis-specific gene discovery in plants: RNA-seq applied to isolated Arabidopsis male meiocytes. *BMC Plant Biology*, **10**, 280.
- Chen, X. (2009) Small RNAs and their roles in plant development. *Annual Review of Cell and Developmental Biology*, **25**, 21–44.
- Cheng, Z., Otto, G.M., Powers, E.N., Keskin, A., Mertins, P., Carr, S.A. *et al.* (2018) Pervasive, coordinated protein-level changes driven by transcript isoform switching during meiosis. *Cell*, **172**, 910–923.
- Crismani, W., Baumann, U., Sutton, T., Shirley, N., Webster, T., Spangenberg, G. *et al.* (2006) Microarray expression analysis of meiosis and microsporogenesis in hexaploid bread wheat. *BMC Genomics*, **7**, 1–17.
- Dai, P., Wang, X., Gou, L.T., Li, Z.T., Wen, Z., Chen, Z.G. *et al.* (2019) A translation-activating function of MIWI/piRNA during mouse spermiogenesis. *Cell*, **179**, 1566–1581.e16.
- Dai, X., Zhuang, Z. & Zhao, P.X. (2018) PsRNATarget: a plant small RNA target analysis server (2017 release). *Nucleic Acids Research*, **46**, W49–W54.
- Dickinson, H.G. & Heslop-Harrison, J. (1977) Ribosomes, membranes and organelles during meiosis in angiosperms. *Philosophical Transactions of the Royal Society of London. Series B, Biological Sciences*, **277**, 327–342.
- Dobin, A., Davis, C.A., Schlesinger, F., Drenkow, J., Zaleski, C., Jha, S. *et al.* (2013) STAR: Ultrafast universal RNA-seq aligner. *Bioinformatics*, **29**, 15–21.
- Dukowicz-Schulze, S., Sundararajan, A., Mudge, J., Ramaraj, T., Farmer, A.D., Wang, M. *et al.* (2014) The transcriptome landscape of early maize meiosis. *BMC Plant Biology*, **14**, 118.
- Engreitz, J.M., Haines, J.E., Perez, E.M., Munson, G., Chen, J., Kane, M. *et al.* (2016) Local regulation of gene expression by lncRNA promoters, transcription and splicing. *Nature*, **539**, 452–455.
- Feng, S., Jacobsen, S.E. & Reik, W. (2010) Epigenetic reprogramming in plant and animal development. *Science*, **330**, 622–627.
- Flórez-Zapata, N.M.V., Reyes-Valdés, M.H. & Martínez, O. (2016) Long non-coding RNAs are major contributors to transcriptome changes in sunflower meiocytes with different recombination rates. *BMC Genomics*, **17**, 1–16.
- Foissac, S. & Sammeth, M. (2007) ASTALAVISTA: dynamic and flexible analysis of alternative splicing events in custom gene datasets. *Nucleic Acids Research*, **35**, 297–299.
- Fultz, D., Choudury, S.G. & Slotkin, R.K. (2015) Silencing of active transposable elements in plants. *Current Opinion in Plant Biology*, **27**, 67–76.
- Geisinger, A., Rodriguez-Casuriaga, R. & Benavente, R. (2021) Transcriptomics of meiosis in the male mouse. *Frontiers in Cell and Developmental Biology*, **9**, 1–14.
- Goh, W.S.S., Falcatori, I., Tam, O.H., Burgess, R., Meikar, O., Kotaja, N. *et al.* (2015) PiRNA-directed cleavage of meiotic transcripts regulates spermatogenesis. *Genes & Development*, **29**, 1032–1044.
- Goldberg, R., Beals, T. & Sanders, P. (1993) Anther development: basic principles and practical applications. *Plant Cell*, **5**, 1217–1229.
- Golicz, A.A., Allu, A.D., Li, W., Lohani, N., Singh, M.B. & Bhalla, P.L. (2021) A dynamic intron retention program regulates the expression of several hundred genes during pollen meiosis. *Plant Reprod.*, **34**, 225–242.
- Gou, L.T., Dai, P., Yang, J.H., Xue, Y., Hu, Y.P., Zhou, Y. *et al.* (2014) Pachytene piRNAs instruct massive mRNA elimination during late spermiogenesis. *Cell Research*, **24**, 680–700.
- Grelon, M., Vezon, D., Gendrot, G. & Pelletier, G. (2001) AtSPO11-1 is necessary for efficient meiotic recombination in plants. *The EMBO Journal*, **20**, 589–600.
- Guo, J.C., Fang, S.S., Wu, Y., Zhang, J.H., Chen, Y., Liu, J. *et al.* (2019) CNIT: a fast and accurate web tool for identifying protein-coding and long non-coding transcripts based on intrinsic sequence composition. *Nucleic Acids Research*, **47**, W516–W522.
- Guo, W., Calixto, C.P.G., Brown, J.W.S. & Zhang, R. (2017) TSIS: an R package to infer alternative splicing isoform switches for time-series data. *Bioinformatics*, **33**, 3308–3310.
- Hawley, B.R., Lu, W.T., Wilczynska, A. & Bushell, M. (2017) The emerging role of RNAs in DNA damage repair. *Cell Death and Differentiation*, **24**, 580–587.
- He, Y., Wang, C., Higgins, J.D., Yu, J., Zong, J., Lu, P. *et al.* (2016) MEIOTIC F-BOX is essential for male meiotic DNA double-strand break repair in rice. *Plant Cell*, **28**, 1879–1893.
- Higgins, J.D., Sanchez-Moran, E., Armstrong, S.J., Jones, G.H. & Franklin, F.C.H. (2005) The Arabidopsis synaptonemal complex protein ZYP1 is required for chromosome synapsis and normal fidelity of crossing over. *Genes & Development*, **19**, 2488–2500.
- Hirano, T. (2002) The ABCs of SMC proteins: two-armed ATPases for chromosome condensation, cohesion, and repair. *Genes & Development*, **16**, 399–414.
- Huang, J., Wang, C., Wang, H., Lu, P., Zheng, B., Ma, H. *et al.* (2019) Meiocyte-specific and AtSPO11-1-dependent small RNAs and their association with meiotic gene expression and recombination. *Plant Cell*, **31**, 444–464.
- The International Wheat Genome Sequencing Consortium (IWGSC). (2018) Shifting the limits in wheat research and breeding using a fully annotated reference genome. *Science*, **361**, eaar7191.
- Jeppsson, K., Kanno, T., Shirahige, K. & Sjögren, C. (2014) The maintenance of chromosome structure: positioning and functioning of SMC complexes. *Nature Reviews. Molecular Cell Biology*, **15**, 601–614.
- Juneau, K., Palm, C., Miranda, M. & Davis, R.W. (2007) High-density yeast-tiling array reveals previously undiscovered introns and extensive regulation of meiotic splicing. *Proceedings of the National Academy of Sciences of the United States of America*, **104**, 1522–1527.

- Kagale, S., Nixon, J., Khedikar, Y., Pasha, A., Provart, N.J., Clarke, W.E. et al. (2016) The developmental transcriptome atlas of the biofuel crop *Camelina sativa*. *The Plant Journal*, **88**, 879–894.
- Kalvari, I., Nawrocki, E.P., Argasinska, J., Quinones-Olvera, N., Finn, R.D., Bateman, A. et al. (2018) Non-coding RNA analysis using the Rfam database. *Current Protocols in Bioinformatics*, **62**, e51.
- Kang, Y.J., Yang, D.C., Kong, L., Hou, M., Meng, Y.Q., Wei, L. et al. (2017) CPC2: a fast and accurate coding potential calculator based on sequence intrinsic features. *Nucleic Acids Research*, **45**, W12–W16.
- Klepikova, A.V., Kasianov, A.S., Gerasimov, E.S., Logacheva, M.D. & Penin, A.A. (2016) A high resolution map of the *Arabidopsis thaliana* developmental transcriptome based on RNA-seq profiling. *The Plant Journal*, **88**, 1058–1070.
- Kuang, Z., Wang, Y., Li, L. & Yang, X. (2019) miRDeep-P2: accurate and fast analysis of the microRNA transcriptome in plants. *Bioinformatics*, **35**, 2521–2522.
- Langfelder, P. & Horvath, S. (2008) WGCNA: an R package for weighted correlation network analysis. *BMC Bioinformatics*, **9**, 559.
- Langmead, B., Trapnell, C., Pop, M. & Salzberg, S.L. (2009) Ultrafast and memory-efficient alignment of short DNA sequences to the human genome. *Genome Biology*, **10**, R25.
- Lardenois, A., Liu, Y., Walther, T., Chalmel, F., Evrard, B., Granovskaia, M. et al. (2011) Execution of the meiotic noncoding RNA expression program and the onset of gametogenesis in yeast require the conserved exosome subunit Rps6. *Proceedings of the National Academy of Sciences of the United States of America*, **108**, 1058–1063.
- Li, A., Liu, D., Wu, J., Zhao, X., Hao, M., Geng, S. et al. (2014) mRNA and small RNA transcriptomes reveal insights into dynamic homeolog regulation of allopolyploid heterosis in nascent hexaploid wheat. *Plant Cell*, **26**, 1878–1900.
- Li, B. & Dewey, C.N. (2011) RSEM: accurate transcript quantification from RNA-seq data with or without a reference genome. *BMC Bioinformatics*, **12**, 323.
- Li, H. (2018) Minimap2: pairwise alignment for nucleotide sequences. *Bioinformatics*, **34**, 3094–3100.
- Lian, J.P., Yang, Y.W., He, R.R., Yang, L., Zhou, Y.F., Lei, M.Q. et al. (2021) Ubiquitin-dependent Argonaute protein MEL1 degradation is essential for rice sporogenesis and phasiRNA target regulation. *Plant Cell*, **33**, 2685–2700.
- Liu, X., Hao, L., Li, D., Zhu, L. & Hu, S. (2015) Long non-coding RNAs and their biological roles in plants. *Genomics, Proteomics Bioinformatics*, **13**, 137–147.
- Lunardon, A., Johnson, N.R., Hagerott, E., Phifer, T., Polydore, S., Coruh, C. et al. (2020) Integrated annotations and analyses of small RNA-producing loci from 47 diverse plants. *Genome Research*, **30**, 497–513.
- Ma, H. (2006) A molecular portrait of *Arabidopsis* meiosis. *Arabidopsis Book*, **4**, 1–39.
- Martin, A.C., Borrill, P., Higgins, J., Alabullah, A., Ramirez-González, R.H., Swarbreck, D. et al. (2018) Genome-wide transcription during early wheat meiosis is independent of synapsis, ploidy level, and the Ph1 locus. *Frontiers in Plant Science*, **8**, 1–19.
- Martinez, G., Panda, K., Köhler, C. & Slotkin, R.K. (2016) Silencing in sperm cells is directed by RNA movement from the surrounding nurse cell. *Nature Plants*, **2**, 16030.
- Mercier, R., Mézard, C., Jenczewski, E., Macaisne, N. & Grelon, M. (2015) The molecular biology of meiosis in plants. *Annual Review of Plant Biology*, **66**, 297–327.
- Ørom, U.A., Derrien, T., Beringer, M., Gumireddy, K., Gardini, A., Bussotti, G. et al. (2010) Long noncoding RNAs with enhancer-like function in human cells. *Cell*, **143**, 46–58.
- Pertea, M., Pertea, G.M., Antonescu, C.M., Chang, T.C., Mendell, J.T. & Salzberg, S.L. (2015) StringTie enables improved reconstruction of a transcriptome from RNA-seq reads. *Nature Biotechnology*, **33**, 290–295.
- Rey, M.D., Martín, A.C., Higgins, J., Swarbreck, D., Uauy, C., Shaw, P. et al. (2017) Exploiting the ZIP4 homologue within the wheat Ph1 locus has identified two lines exhibiting homeologous crossover in wheat-wild relative hybrids. *Molecular Breeding*, **37**, 95.
- Schmid, R., Grellscheid, S.N., Ehrmann, I., Dalglish, C., Danilenko, M., Paronetto, M.P. et al. (2013) The splicing landscape is globally reprogrammed during male meiosis. *Nucleic Acids Research*, **41**, 10170–10184.
- Sears, E.R. (1977) An induced mutant with homeologous pairing in common wheat. *Canadian Journal of Genetics and Cytology*, **19**, 585–593.
- Serra, H., Svčina, R., Baumann, U., Whitford, R., Sutton, T., Bartoš, J. et al. (2021) Ph2 encodes the mismatch repair protein MSH7-3D that inhibits wheat homeologous recombination. *Nature Communications*, **12**, 1–10.
- Shunmugam, A.S.K., Bollina, V., Dukowic-Schulze, S., Bhowmik, P.K., Ambrose, C., Higgins, J.D. et al. (2018) MeioCapture: an efficient method for staging and isolation of meiocytes in the prophase I sub-stages of meiosis in wheat. *BMC Plant Biology*, **18**, 1–12.
- Springer, N.M., Lisch, D. & Li, Q. (2015) Creating order from chaos: epigenome dynamics in plants with complex genomes. *Plant Cell*, **28**, 314–325.
- Stapley, J., Feulner, P.G.D., Johnston, S.E., Santure, A.W. & Smadja, C.M. (2017) Variation in recombination frequency and distribution across eukaryotes: patterns and processes. *Philosophical Transactions of the Royal Society B: Biological Sciences*, **372**, 20160455.
- Statello, L., Guo, C.J., Chen, L.L. & Huarte, M. (2021) Gene regulation by long non-coding RNAs and its biological functions. *Nature Reviews. Molecular Cell Biology*, **22**, 96–118.
- Taylor, D.H., Chu, E.T.J., Spektor, R. & Soloway, P.D. (2015) Long non-coding RNA regulation of reproduction and development. *Molecular Reproduction and Development*, **82**, 932–956.
- Tock, A.J., Holland, D.M., Jiang, W., Osman, K., Sanchez-Moran, E., Higgins, J.D. et al. (2021) Crossover-active regions of the wheat genome are distinguished by DMC1, the chromosome axis, H3K27me3, and signatures of adaptation. *Genome Research*, **31**, 1614–1628.
- Toufighi, K., Brady, S.M., Austin, R., Ly, E. & Provart, N.J. (2005) The botany array resource: e-Northern, expression angling, and promoter analyses. *The Plant Journal*, **43**, 153–163.
- Trans Decoder. (2018). <https://github.com/TransDecoder/TransDecoder> [Accessed 5th October 2021].
- Tseng, Y., Kole, T.P., Lee, J.S.H., Fedorov, E., Almo, S.C., Schafer, B.W. et al. (2005) How Actin crosslinking and bundling proteins cooperate to generate an enhanced cell mechanical response. *Biochemical and Biophysical Research Communications*, **334**, 183–192.
- Wagner, G.P., Kin, K. & Lynch, V.J. (2012) Measurement of mRNA abundance using RNA-seq data: RPKM measure is inconsistent among samples. *Theory in Biosciences*, **131**, 281–285.
- Walker, J., Gao, H., Zhang, J., Aldridge, B., Vickers, M., Higgins, J.D. et al. (2018) Sexual-lineage-specific DNA methylation regulates meiosis in *Arabidopsis*. *Nature Genetics*, **50**, 130–137.
- Wang, K.C., Yang, Y.W., Liu, B., Sanyal, A., Corces-Zimmerman, R., Chen, Y. et al. (2011) A long noncoding RNA maintains active chromatin to coordinate homeotic gene expression. *Nature*, **472**, 120–126.
- Wang, L., Xu, Z., Khawar, M.B., Liu, C. & Li, W. (2017) The histone codes for meiosis. *Reproduction*, **154**, R65–R79.
- Wang, Y., Cheng, Z. & Ma, H. (2014) Meiosis: interactions between homologous chromosomes. In: Assmann, S. & Liu, B. (Eds.), *Cell Biology*. New York, NY: Springer, pp. 1–34.
- Winter, D., Vinegar, B., Nahal, H., Ammar, R., Wilson, G.V. & Provart, N.J. (2007) An “electronic fluorescent pictograph” browser for exploring and analyzing large-scale biological data sets. *PLoS One*, **2**, 1–12.
- Yang, H., Lu, P., Wang, Y. & Ma, H. (2011) The transcriptome landscape of *Arabidopsis* male meiocytes from high-throughput sequencing: the complexity and evolution of the meiotic process. *The Plant Journal*, **65**, 503–516.
- Yates, A.D., Achuthan, P., Akanni, W., Allen, J., Allen, J., Alvarez-Jarreta, J. et al. (2020) Ensembl 2020. *Nucleic Acids Research*, **48**, D682–D688.
- Zhou, Y., Zhou, B., Pache, L., Chang, M., Khodabakhshi, A.H., Tanaseichuk, O. et al. (2019) Metascape provides a biologist-oriented resource for the analysis of systems-level datasets. *Nature Communications*, **10**, 1–10.
- Zickler, D. & Kleckner, N. (2015) Recombination, pairing, and synapsis of homologs during meiosis. *Cold Spring Harbor Perspectives in Biology*, **7**, a016626.